PRAMANA
— journal of
physics

© Indian Academy of Sciences

Vol. 75, No. 1
July 2010
pp. 25–38

Structure of $A\sim130$ nuclei in La–Ce region

TUMPA BHATTACHARJEE
Variable Energy Cyclotron Centre, 1/AF, Bidhan Nagar, Kolkata 700 064, India
E-mail: btumpa@veccal.erent.in

Abstract. The variety of shapes and structures, observed in light rare earth $A\sim130$ nuclei, have been discussed in view of different angular momentum coupling schemes and their interplay that comes into effect at high spin. The $N = 79$ and 80 isotopes in La–Ce region, produced via fusion evaporation reaction, have been studied using the Indian National Gamma Array (INGA) consisting of 18 clover HPGe detectors. Two nearly degenerate $\Delta I = 1$ bands have been observed at high spin of ^{137}Ce and a triaxial deformation of $\gamma = \pm30^\circ$ has been assigned to the bands, from the total Routhian surface (TRS) calculations. The high-spin candidates of the yrast band of ^{138}Ce show signature splitting both in energy and $B(M1)/B(E2)$ values. The bandcrossing due to the alignment of a pair of $h_{11/2}$ proton particles has been conjectured at $\hbar\omega \sim 0.3$ MeV, from the single-particle Routhians obtained from TRS calculations. Lifetime measurements by Doppler shift attenuation method (DSAM) has been carried out and from the estimated reduced transition probability $B(M1)$, the $\Delta I = 1$ band in ^{138}Ce has been characterized as a magnetic rotation (MR) band. The rise in the values of $B(M1)$, for the higher spin candidates of the band, has been conjectured as the reopening of a different shear at the top of the Band B1. The characteristic of the MR bands in $A \sim 130$ region has been discussed in the light of a phenomenological calculation and compared to the MR bands in other mass regions.

Keywords. Clover detector array; measured E_γ, I_γ, DCO (directional correlation of oriented states), polarization; lifetime measurement with Dopper shift attenuation method; reduced transition probability $B(M1)$; shell model; Tilted Axis Cranking calculation; total Routhian surface calculations; backbending; magnetic rotation bands.

PACS Nos 21.10.-k; 23.20.-g; 27.60.+j

1. Introduction

The rich variety in the shapes and structures arising out of different angular momentum coupling schemes, observed in the light rare-earth nuclei with $50 \leq N(Z) \leq 82$, have attracted considerable experimental interest in recent years. The systematic study of different band structures, viz., chiral bands, magnetic rotation bands, highly deformed band etc., has revealed that the multiparticle excitation to $h_{11/2}$ orbitals and alignments of the $h_{11/2}$ quasiparticles play an important role, even at very high excitation energies of these nuclei. The low-lying structure of almost all the nuclei in this mass region, on the contrary, is contributed mainly by the

excitation of one or a few proton particles to the $d_{5/2}$ and/or $g_{7/2}$ orbitals and one or a few neutron holes to the $h_{11/2}$ orbital that can be reasonably explained in the shell model framework. Such an evolution from single particle to a superdeformed structure, via stable triaxial shapes, has been observed recently in the even–even ^{140}Nd nucleus [1]. The observed varieties in shapes at high spin are introduced in these nuclei, because of the competing shape driving effects of the high-j high-Ω neutron $h_{11/2}$ holes and the high-j low-Ω proton $h_{11/2}$ particles. The rotational alignment, along the axis of rotation, of a pair of $h_{11/2}$ neutrons, gives rise to an oblate shape [2], whereas that of a $h_{11/2}$ proton pair gives rise to a prolate shape [3] in these γ-soft nuclei. Both the alignments, giving rise to a shape-coexistence, have been observed in the odd–odd ^{131}La [3]. The $A \sim 130$ nuclei having γ-soft cores are, therefore, one of the best testing examples for studying the evolution of triaxial shapes. Experimental data on the odd–odd and odd-A nuclei of this mass region have also displayed a varied amount of signature splitting in the yrast sequence and in many cases, signature inversion of quasiparticle Routhians has been observed. These have been attributed as the fingerprints of triaxiality in nuclei, by cranked shell-model calculation [4]. The observation of two nearly degenerate $\Delta I = 1$ bands, known as the chiral bands, in the odd–odd [5] and odd-A [6] nuclei of this mass region, have established the presence of a different orientation geometry of the deformed nuclear mean field and the coupling of the extra-core odd particles. As evidenced from the experimental signatures and understood from theoretical calculations, in such cases, the angular momentum of the triaxially deformed core is perpendicular to the individual angular momenta of both the odd particles. In many of the odd–odd cases [7], the chiral vibration due to the tunnelling between two chiral minima have been observed. Bands with stable triaxial minima, arising due to excitation of neutron quasiparticles beyond the $N = 82$ shell gap, has been predicted from cranked Nilsson–Strutinsky calculations and subsequently observed in several Nd isotopes as well, e.g., in ^{139}Nd [8], at an excitation energy of $\sim$10 MeV. Along with all these phenomena, depicting deformation in a nucleus, rotation-like sequences of strongly enhanced magnetic dipole ($M1$) transitions, observed in spherical or near-spherical nuclei of this mass region, have drawn considerable interest in recent years. These are known as magnetic rotation (MR) bands [9] and the high-spin states of these bands are generated by the gradual alignment of the proton and neutron spin vectors ($\vec{j}_\pi$ and $\vec{j}_\nu$) along the direction of the total angular momentum $\vec{I}$. This step-by-step alignment resembles the closing of a pair of blades of a shear and hence this mechanism of generating angular momentum is popularly termed as the 'shears mechanism'. The characteristics of these bands are exhibited in rotation-like $I(I+1)$ pattern, with a relatively low dynamic moment of inertia ($J(2)$) and large $B(M1)/B(E2)$ ratios, in spite of very low deformation in the nucleus. For these bands, the perpendicular component of the dipole moment ($\mu_\perp$) and, therefore, the $B(M1)$ values decrease in a characteristic manner with the increase in angular momentum I. The understanding of the mechanism of angular momentum coupling, involved in the MR bands, has been realized by using Tilted Axis Cranking Model [10]. The semiclassical prescription, suggested by Clark and Macchiavelli [11], where experimental observables like spin, excitation energy, moment of inertia, alignments and reduced transition probabilities can be described as functions of the angle, known as the 'shear angle', among the proton

and neutron blades, has been quite successful in understanding the MR bands in $A \sim 200$ as well as in $A \sim 110$ regions.

In this paper, the experimental results and the theoretical interpretation will be presented on odd–odd ^{136}La, odd-A ^{137}Ce and even–even ^{138}Ce. The said nuclei have been studied using the Indian National Gamma Array (INGA) facility. The results will be discussed in the light of the observed variety in their high-spin structure. A systematic analysis of the MR bands in $A \sim 130$ region has been done using the above semiclassical model in order to compare their features with similar bands from other mass regions.

2. Experiment and analysis

The ^{136}La nucleus was populated at 14UD BARC-TIFR Pelletron Facility by using the fusion evaporation reaction ^{130}Te(^{11}B,5$n\gamma$) at $E_{\rm beam} = 52$ MeV. The target used was a 2.2 mg/cm^2 enriched (99.9%) ^{130}Te, evaporated on a 2 mg/cm^2 gold backing. The γ-rays were detected by the early implementation of INGA array, consisting of eight clover Ge detectors. The eight detectors were arranged in the median plane at $\pm 30°$, $60°$, $90°$, $120°$, $-70°$, $-105°$ and $-145°$ angles with respect to the beam direction. Around 260 million events were recorded in compressed list mode using the multiparameter CAMAC-based data acquisition system LAMPS [12]. The data have been analysed for extracting the γ–γ and γ–γ–γ coincidences, DCO and polarization information. The detailed level scheme along with the theoretical interpretation will be found in ref. [13].

The high-spin states of ^{137}Ce [14] and ^{138}Ce [15] nuclei were produced via ^{130}Te(^{12}C,xn) reaction at $E_{\rm beam} = 63$ MeV at 15UD Pelletron of Inter-University Accelerator Centre, New Delhi. The main emphasis of the present experiment was to measure the lifetimes of the excited levels of ^{138}Ce by DSAM technique. A thin (800 μg/cm^2) target with a thick (4.8 mg/cm^2) Au backing was used so that most of the recoiling nuclei stop in the backing material. In this experiment, 18 detectors were placed on the support structure in five different rings around the target chamber, out of which five detectors were available in the $90°$ ring, four in $57°$ and the rest were placed in groups of three in $32°$, $123°$ and $148°$ respectively. Around 1.4 billion three- and higher-fold Compton-suppressed coincidence events have been gathered. The data were sorted into different matrices corresponding to different angles using the modified version of INGASORT [16], with a view to look for the lineshapes in the γ-ray peaks belonging to ^{138}Ce and ^{137}Ce. The projected spectra show lineshapes in the γ-ray lines of the $\Delta I = 1$ band B1 and yrast band B2 of ^{138}Ce [15]. Figure 1 shows the 664.5 keV γ-ray of band B1, as observed in detectors, placed at different angles, along with the lineshapes, fitted using the LINESHAPE code [17]. The geometries of the clover detectors have been taken into account while generating the time-dependent velocity profile of the recoil, required for the fitting of the observed lineshapes. The deduced lifetimes have been used to calculate the transition probabilities of different levels.

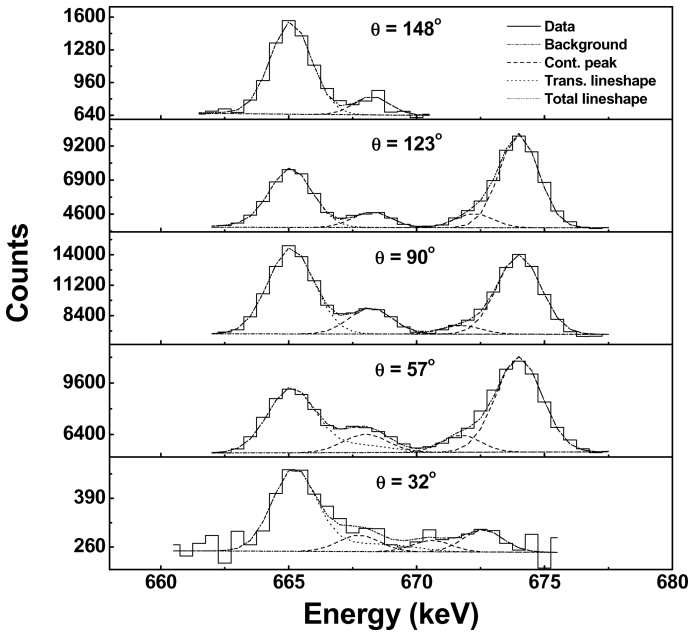

Figure 1. Lineshape for the 664.5 keV γ-rays depopulating the Band B1 of ^{138}Ce. In the figure, the solid line represents the experimental data, dotted line represents the fitted lineshape for the transition of interest and the dash—dot–dot line shows the total lineshape. The background has been drawn with the dash–dot line and the dashed lines show the extra stopped peaks.

3. Results and discussion

The main features in the structure of the odd–odd ^{136}La, odd-A ^{137}Ce and even–even ^{138}Ce will be discussed in the following subsections along with the systematic study that has been performed for a few nuclei in this mass region.

3.1 *$N = 79$ ^{136}La and neighbouring odd–odd nuclei*

The low-lying levels of the odd–odd nuclei in La–Ce region depict the presence of proton–neutron multiplet states, governed by the available single-particle states and the underlying residual interactions between them. At high-spin, semidecoupled bands with small staggering have been observed in these nuclei [18,19], having underlying configuration, such as, $\pi h_{11/2} \otimes \nu h_{11/2}$. These bands are generally yrast in nature and are built on the characteristic long-lived isomeric state, systematically present in these nuclei. The yrast band of ^{136}La has been established to have the same multiparticle configuration which could be well explained with a particle rotor model calculation [13]. It is evident from a systematic comparison of the level energies of the yrast bands of the $N = 79$ ^{134}Cs, ^{136}La, ^{138}Pr and ^{140}Pm nuclei that, with the addition of extra protons, the $\pi h_{11/2} \otimes \nu h_{11/2}$ band structure gets

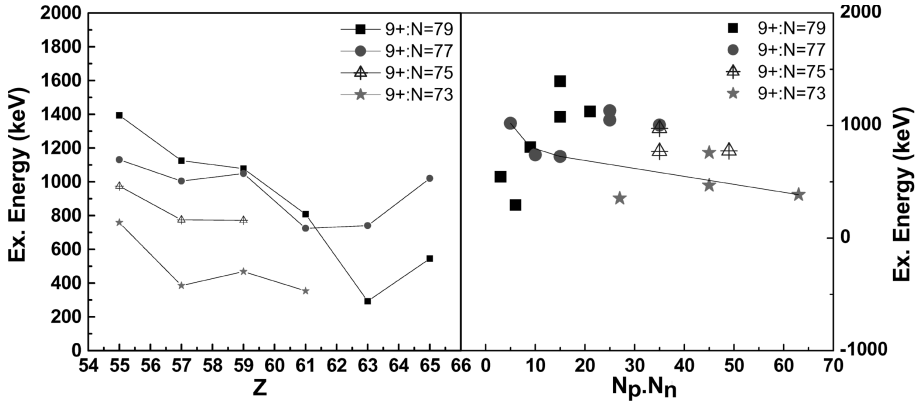

Figure 2. The plot of excitation energies of the 9^+ states of the $\pi h_{11/2} \otimes \nu h_{11/2}$ bands vs. Z (left panel) and $N_p \cdot N_n$ (right panel) respectively.

diluted at high spin whereas, the structure becomes more irregular as one moves towards $Z = 55$. In figure 2, the excitation energies of the 9^+ states, belonging to the said band structure of the odd–odd nuclei, have been shown with respect to the atomic number Z as well as the product of valence proton and valence neutron $(N_p \cdot N_n)$. The increase in the excitation energy as one goes towards $Z = 55$ as well as the irregular nature of the level structure for the $Z = 55$ isotone indicate the likely effect of a subshell closure at $Z = 56$. The experimental study of the band structures in the odd–odd nuclei below ^{134}Cs is, therefore, required in order to confirm such evidences.

3.2 *Even-Z, odd-A* ^{137}*Ce*

In even-Z odd-A nuclei around $A \sim 130$ region, there exists a band structure, built on $\frac{11}{2}^-$ isomer, that can be explained by invoking a weak-coupling picture in which an odd neutron in $h_{11/2}$ orbital is coupled to the underlying even–even core. Such a weak coupling picture is respected up to a moderate spin and excitation energy for the nuclei which are not far from $N = 82$ shell closure. Figure 3 shows the systematics of such states in odd-A Ce isotopes including $N = 79$ ^{137}Ce. It is evident that as one approaches $N = 82$ shell closure the agreement is quite well even for the high-spin members.

The high-spin level scheme of $N = 79$, ^{137}Ce [14] consists of several band-like structures, including two $\Delta I = 1$ bands, viz. Band 6, developed on the 5379.1 keV $\frac{33}{2}^+$ state and Band 4, developed on $\frac{31}{2}^+$ state at 4225 keV level, as shown in figure 4, that are connected by $M1 + E2$ transitions. As is evident from the above figure, these two bands are separated by ∼600 keV near the respective band heads and becomes almost degenerate as they approach the highest observed spin. The TRS calculation [20–22] has been performed by considering different 5-qp configurations in order to interpret Bands 6 and 4. The configuration

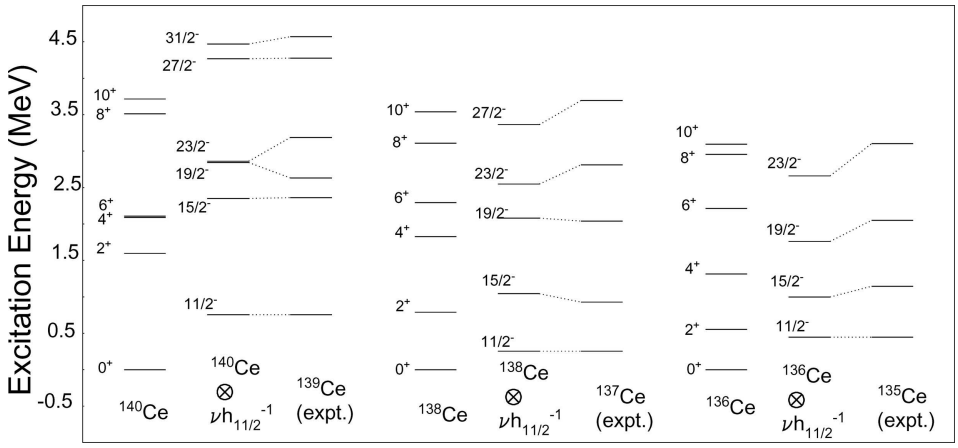

Figure 3. Systematics of the core-coupled states in the odd-A Ce isotopes.

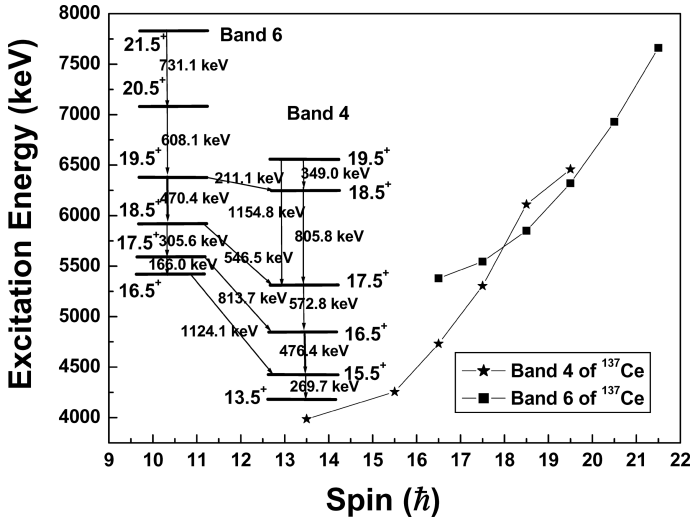

Figure 4. The plot of excitation energies of the Bands 4 and 6 of ^{137}Ce with respect to the angular momentum I. The two bands have been shown in the inset.

$\pi(+,+1/2)(-,+1/2)\nu(+,+1/2)^2(-,+1/2)$, gives rise to positive parity band with two consistent deformation minima at $\gamma = \pm 30°$, present throughout the range of the considered ω values. The Routhian plots for the two minima cross each other at an ω value very close to the band head frequency, as shown in figure 5. It has been observed that the Routhian for the $+30°$ minima matches well with the experimental data of Band 6 and that for $-30°$ minima matches well with the experimental data of Band 4. So, these two bands, predicted to have a triaxial deformation, show degeneracy in the level energy at high spin. These two bands

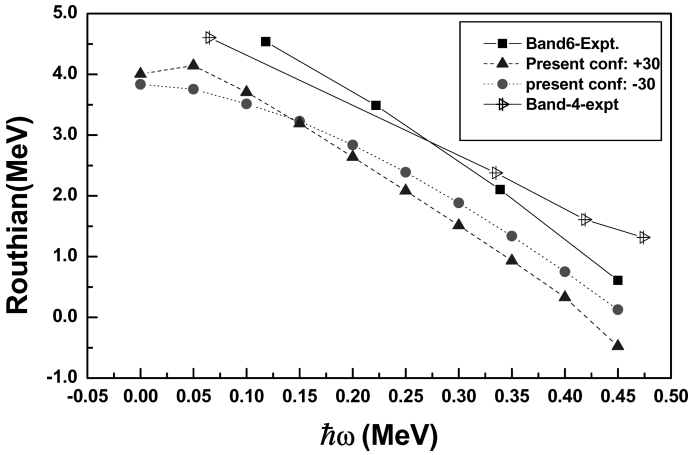

Figure 5. The plot of experimental Routhians for Bands 4 and 6 of ^{137}Ce with respect to angular frequency ω. The theoretical Routhians obtained from the cranking calculation have also been shown.

may thus form a chiral pair and the measurement of the transition probabilities as well as the interpretation with tilted axis cranking codes will be necessary to establish the same.

3.3 *Even–even* $N = 80$ ^{138}*Ce*

The even–even ^{138}Ce with $Z = 58$ and $N = 80$ is a near spherical nucleus, in which, according to shell model, the eight protons outside the $Z = 50$ closed shell fill the $g_{7/2}$ orbital making the proton excitation to $h_{11/2}$ less favoured, energetically. Therefore, one observes a dominance of neutron hole excitation in this nucleus at low excitation. Besides, one observes 7^- and 10^+ isomers at a modest excitation energy which arise due to different two-neutron hole configurations. A reasonable agreement has been observed between the shell model calculations and the experimental data for the medium spin positive and negative parity states below 6 MeV, in the yrast band of ^{138}Ce (see figure 6 for positive parity states). The calculation was done in the proton–neutron formalism with ^{100}Sn as a core, using the code OXBASH [23,24], the details of which are given in ref. [15].

The major configuration of the states has been found to be $[\pi(g^6_{7/2}d^2_{5/2}) \otimes \nu h^{-2}_{11/2} + \pi(g^5_{7/2}d^3_{5/2}) \otimes \nu h^{-2}_{11/2}]$ for positive parity and $[\pi(g^6_{7/2}d^1_{5/2}h^1_{11/2}) \otimes \nu h^{-2}_{11/2} + \pi(g^5_{7/2}d^2_{5/2}h^1_{11/2}) \otimes \nu h^{-2}_{11/2} + \pi(g^5_{7/2}d^3_{5/2}) \otimes \nu(s^{-1}_{1/2}h^{-1}_{11/2})]$ for negative parity states.

For the higher spin states above 6 MeV excitation, the level structure is significantly fragmented into different bands. The observed signature splitting above $14\hbar$, as shown in figure 7, is characteristic of a typical situation, where the Fermi levels lie in the middle or upper half of a high-j orbital and indicates the onset of deformation and a change in shape beyond 14^+ [25,26].

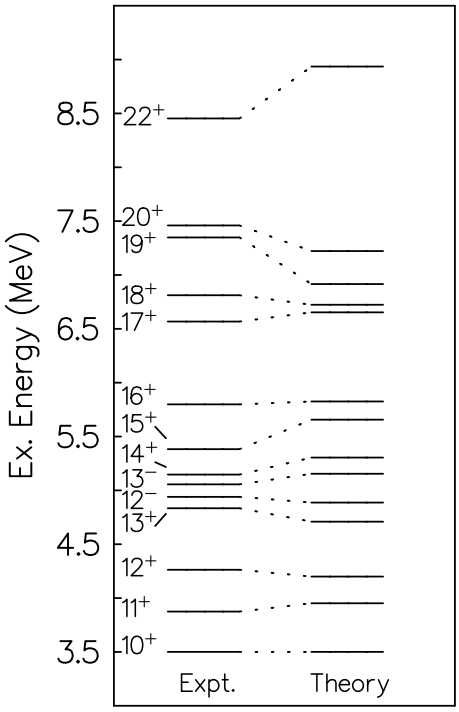

Figure 6. Plot of the results obtained from the shell model calculations for the cascade B2. Experimental levels have been shown for comparison.

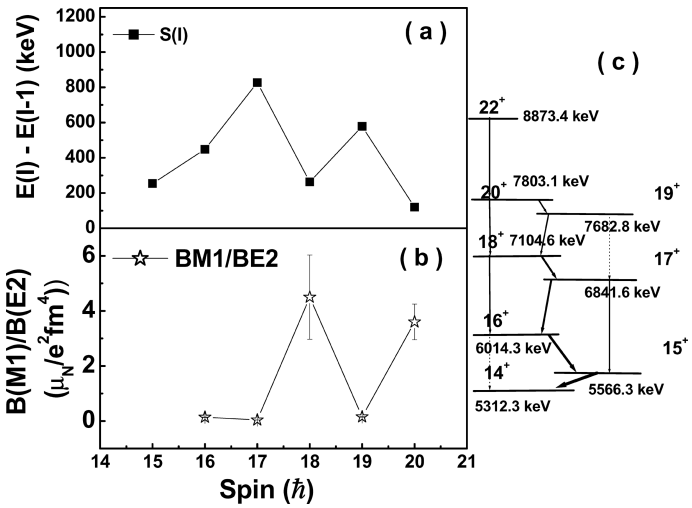

Figure 7. The observed signature splitting in (**a**) energy and (**b**) transition probability for the yrast band B2 of ^{138}Ce. The part of the band has been shown in (**c**).

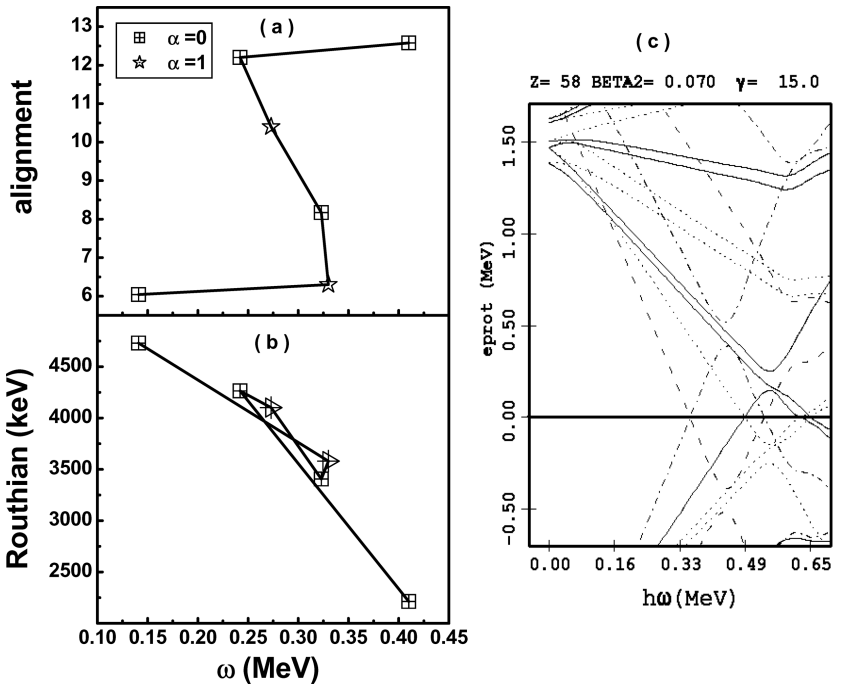

Figure 8. The experimental (**a**) alignment and (**b**) Routhian for the high-spin candidates of Band B2 of ^{138}Ce has been plotted with angular frequency ω. The single-particle Routhian as obtained from TRS calculation has been shown in (**c**).

A sudden increase in the alignment (i') and a sudden change in the Routhian, as shown in figures 8a and 8b, indicate the excitation of a pair of quasiparticles at an angular frequency $\omega \sim 0.3$. The single-particle Routhians obtained from the TRS calculation has been shown in figure 8c and such crossing is observed at similar frequency in the negative parity $h_{11/2}$ orbital in the proton space. Thus the splitting of energy and transition probability in the yrast Band B2 is interpreted to be arising out of an alignment of a pair of $h_{11/2}$ proton quasiparticles, inducing a significant deformation in the band. Accordingly, a 4-quasiparticle configuration for the positive parity band above 6 MeV, such as $\pi h_{11/2}^2 \otimes \nu h_{11/2}^{-2}$, is suggested.

The band sequence B1 of ^{138}Ce, shown in figure 9a, has been established to be a $\Delta I = 1$ negative parity sequence, built on the 15^- state at 6536.3 keV. From the systematics of the MR bands in the neighbouring Ce isotopes, the configuration for Band B1 is proposed to be $\pi h_{11/2} g_{7/2} \otimes \nu h_{11/2}^{-2}$. A semiempirical calculation with this proposed configuration has been able to identify well the structure as a magnetic rotation band [15]. The reduced transition probability $B(M1)$ for Band B1 has been extracted from the measured lifetimes of the excited levels, as described in §2. The $B(M1)$ values are plotted against the angular momentum I in figure 9b. The plot depicts a decreasing trend in the reduced transition probability as one goes higher in angular momentum along Band B1, upto spin $20\hbar$. Such a characteristic

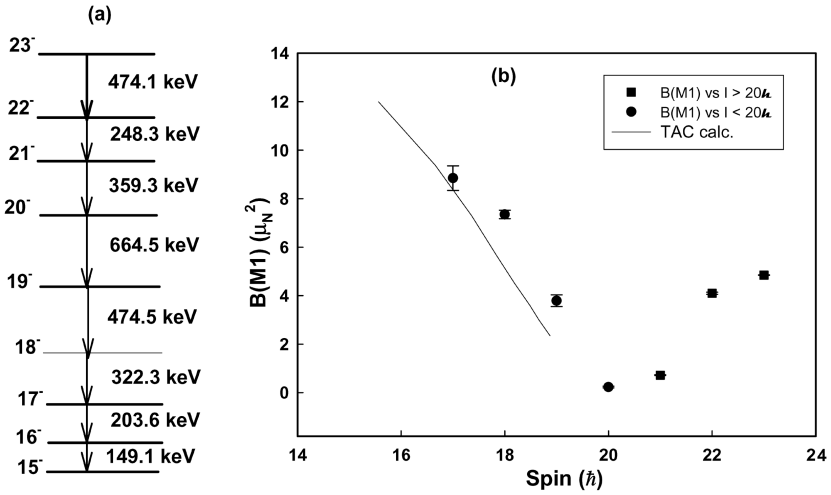

Figure 9. (**a**) The Band B1 of ^{138}Ce. (**b**) The $B(M1)$ values for the band has been plotted with respect to the angular momentum I. The solid line shows the result from TAC calculations.

drop in the $B(M1)$ values along the band confirms Band B1 as an MR band. But, beyond spin $20\hbar$, the $B(M1)$ values increase subsequently for the top three levels of the same band. Similar increase in $B(M1)$ values were observed in ^{197}Pb nucleus [27] and was attributed to a reopening of the shears with a different configuration. Similar reopening of shears is also conjectured for the present case from the tilted axis calculation and semiempirical description [28].

3.4 *Systematics of MR bands in the mass ∼130 region*

Following the discovery of the shears mechanism in the mass ∼190 region, there have been experimental efforts to search for similar mechanism in other mass regions. According to a recent compilation of MR bands [29,30], there exist quite a few cases in the light rare-earth nuclei. Ideally, the MR bands are developed purely out of the shears mechanism, though a contribution from core rotation may be important, as has been observed in the case of MR bands in the mass ∼130 region. Here, a systematic study of the shears bands, observed in the even–even nuclei in the mass ∼130 region, will be attempted along with the one in ^{138}Ce (see §3.3). The experimental details of the bands with their configurations, taken from refs [29,30], except for Band B1 of ^{138}Ce, are listed in table 1.

According to Clark and Macchiavelli [11], the shears mechanism in its barest form is described by the coupling of two long angular momentum vectors $\vec{j}_\pi$ and $\vec{j}_\nu$ to the total angular momentum $\vec{I}$ of the shears band. The shears angle θ (angle between the vectors $\vec{j}_\pi$ and $\vec{j}_\nu$) is one of the important degrees of freedom in describing the properties of the band and is derived by using the semiclassical expression [35]:

$$\cos\theta = \frac{\vec{j}_\nu \cdot \vec{j}_\pi}{|\vec{j}_\nu||\vec{j}_\pi|} = \frac{I_{\rm shears}(I_{\rm shears}+1) - j_\nu(j_\nu+1) - j_\pi(j_\pi+1)}{2\sqrt{j_\nu(j_\nu+1)j_\pi(j_\pi+1)}}, \quad (1)$$

where $I_{\rm shears}$ is the angular momentum generated out of the shears mechanism and can be obtained by subtracting the contribution of core rotation ($R_{\rm core}$) from the observed angular momentum I as

$$\vec{I}_{\rm shears} = \vec{I} - \vec{R}_{\rm core},$$

where

$$R_{\rm core} = \frac{\Delta R}{\Delta I}(I - I_{\rm bandhead})$$

and

$$\frac{\Delta R}{\Delta I} \approx \frac{[I_{\rm max} - (j_\pi + j_\nu)]}{(I_{\rm max} - \sqrt{j_\pi^2 + j_\nu^2})}.$$

The rotational contributions in the topmost levels of the bands have been calculated and are listed in table 1 along with the observed spin. Assuming that the interaction between the nucleons forming each blade is independent of the shears angle θ, the energy needed to form the blades is contained within the energy of the bandhead. In cases where almost all the total angular momentum along the entire spin range of the band is generated through the shears mechanism, a reasonable approximation can be made that the excitation energy along the band arises only by the change in potential energy caused by the recoupling of the two angular momentum vectors, $\vec{j}_\pi$ and $\vec{j}_\nu$, so that

$$V_{\pi\nu}[I(\theta)] = E(I) - E_{\rm bandhead} = E_x. \quad (2)$$

The nature of the effective p-n interaction ($V_{\pi\nu}$) between the nucleons, involved in the shears mechanism, is a function of the shears angle θ. By neglecting the higher-order terms, $V_{\pi\nu}$ can be expanded in even multipoles [35] as

Table 1. Contribution from rotation in the topmost level of the shears band in the even–even nuclei in mass 130 region.

Nucleus	Configuration	Contribution of rotation at the topmost level (level spin)
^{132}Ba(B3) [31] (B2) [32]	$\pi h_{11/2}g_{7/2} \otimes \nu h_{11/2}d_{3/2}$	11% (18)
^{132}Ba(B9) [31] (B3) [32]	$\pi h_{11/2}g_{7/2} \otimes \nu h^{-2}_{11/2}$	5% (20)
^{134}Ce [33]	$\pi h_{11/2}g_{7/2} \otimes \nu h^{-2}_{11/2}$	5% (20)
^{136}Ce(B5) [34]	$\pi h^{-2}_{11/2} \otimes \nu h^{-2}_{11/2}$	5% (19)
^{136}Ce(B6) [34]	$\pi h_{11/2}g_{7/2} \otimes \nu h_{11/2}g_{7/2}$	13% (23)
^{136}Ce(B3) [34]	$\pi h_{11/2}g_{7/2} \otimes \nu h^{-2}_{11/2}$	17% (23)
^{138}Ce [15]	$\pi h_{11/2}g_{7/2} \otimes \nu h^{-2}_{11/2}$	5% (20)

Table 2. The interaction strength of the shears (V_2) and χ values in the MR bands in the even–even nuclei in the mass 135 region.

Nucleus	V_2 per p–n pair (keV)	χ (fit)
^{132}Ba [B3(B2)]	410	0.12(0.04)
^{132}Ba [B9(B3)]	407	0.1(0.01)
^{134}Ce (B5)	454	0.1(0.01)
^{136}Ce (B5)	436	0.1(0.01)
^{136}Ce (B6)	521	0.24(0.04)
^{136}Ce (B3)	682	0.32(0.04)
^{138}Ce (B1)	386	0.09(0.002)
^{198}Pb	300	
^{110}Cd	500	

$$V_{\pi\nu}[I(\theta)] = V_0 + V_2 P_2(\cos\theta). \tag{3}$$

The significant part of the interaction strength comes from the term $V_2 P_2(\cos\theta)$ in which V_2 would be positive for a particle–hole configuration of the shears band. The parameters V_0 and V_2 have been extracted by a least-squares fit of function (3) to the experimental data points for several nuclei in the mass ∼130 region. It is seen that the interaction strengths can be well represented by a $P_2(\cos\theta)$ dependence, similar to that obtained in $A \sim 190$ region. The interaction strength per proton(particle)–neutron(hole) pair have been obtained systematically, for all the nuclei, and compared with those obtained from the mass ∼110 and 190 region (table 2).

The competition between the shears mechanism and the rotation of the core has been estimated by adding a rotational energy term ($R^2/2\Im$) to the excitation energy of the band, following ref. [36], i.e.,

$$\begin{aligned} E(I) &= \frac{R^2}{2\Im} + V_2 P_2(\theta) \\ &= \frac{(\vec{I} - \vec{j}_\pi - \vec{j}_\nu)^2}{2\Im} + V_2 P_2(\theta), \end{aligned} \tag{4}$$

where I is the observed angular momentum and $\Im$ = moment of inertia of the core. The above equation can be solved in the classical limit with the minimization condition $(\partial E/\partial\theta)_I = 0$ to obtain

$$I_{\rm red} = \cos\left(\frac{\theta}{2}\right)(1 + \chi\cos\theta) \tag{5}$$

in which $I_{\rm red} = I/(j_\pi + j_\nu)$ and $\chi = \Im/(j^2/3V_2) = \Im/\Im_{\rm eff}$ is a dimensionless parameter with $\Im_{\rm eff}$ being the effective moment of inertia of the shears. The parameter χ, thus, is a measure of the relative strength between the shears mechanism and the rotation of the core. When $\chi \to 0$, the contribution of the core rotation almost vanishes and the system prefers to generate the angular momentum by shears mechanism only, whereas, when $\chi \to \infty$, the rotation of the core dominates. For some

of the bands, the shears angle (θ) as a function of the reduced spin ($I_{\rm red}$) has been plotted and the data points have been fitted with expression (5) to obtain the value of the parameter χ for all the bands which are tabulated in column 3 of table 2. This value comes out to be ∼0.09, for Band B1 of ^{138}Ce, which is well within the limit of a shears band. It is observed that the Bands B3, B6 of ^{136}Ce and the Band B3 of ^{132}Ba have the χ values very close to 0.5, implying a significant contribution from rotation, and is corroborated by the numbers in table 1. On the contrary, the bands in ^{134}Ce and ^{138}Ce, Band B2 in ^{132}Ba and the Band B5 in ^{136}Ce have χ values ∼0.1 indicating the dominance of shears mechanism for the said bands. It may, therefore, be concluded that the core rotation plays an important role in the MR bands of the mass ∼130 region.

4. Summary

The nuclei close to $N = 82$ shell closure have been studied using the Indian National Gamma Array. The systematic investigation of the high-spin structure of the odd–odd nuclei in the La–Ce region has been carried out and the evidence of the $Z = 56$ shell closure has been observed from the systematic comparison of the $\pi h_{11/2} \otimes \nu h_{11/2}$ structure of the yrast band in these nuclei. The odd-A^{137}Ce nucleus reflects a core-coupled picture at low spin, whereas, at high spin two $\Delta I = 1$ bands have been observed and these two bands have been conjectured as the possible chiral partner. The yrast structure of the even–even ^{138}Ce nucleus has been reproduced with a shell model calculation at low spin and on the contrary, the high-spin structure depicts a signature splitting in its energy and transition probability and a band crossing has been predicted in this band at $\omega \sim 0.33$ MeV from the single-particle Routhians obtained from principal axis cranking calculation. The $\Delta I = 1$ band in ^{138}Ce has been predicted as a magnetic rotation band from the measurement of lifetimes of the levels with DSAM technique. The reopening of a new shear has been predicted from the rise in $B(M1)$ values of this band above spin $20\hbar$. The systematic comparison of the MR bands have been done in the light of semiempirical description and it has been observed that the rotational contribution is sizable in many of the MR bands in La–Ce region. However, the MR band in ^{138}Ce has been found to be an ideal shear band with a very negligible contribution from rotation. The interaction strength V_2 has been calculated for the MR bands of $A \sim 130$ region and it has been found that the interaction strength is less for the MR bands in this mass region compared to $A \sim 200$ and ∼110 mass regions.

Acknowledgements

The author would like to acknowledge the meaningful collaboration with all her collaborators from VECC, SINP, UGC-DAE-CSR, CU, BARC and IUAC. The author is specially thankful to Prof. A O Machiavelli for very useful discussions regarding the semiclassical analysis of MR bands. The effort of BARC-TIFR and IUAC pelletron staff members for the smooth running of the machine and the INGA Collaboration for setting up the array is acknowledged with thanks.

References

[1] C Petrache *et al*, *Phys. Rev.* **C68**, 064318 (2005)
[2] E S Paul *et al*, *Nucl. Phys.* **A619**, 177 (1997)
[3] E S Paul *et al*, *Phys. Rev. Lett.* **58**, 984 (1987)
[4] R Bengtsson *et al*, *Nucl. Phys.* **A415**, 189 (1984)
[5] V I Dimitrov, S Frauendorf and S Donau, *Phys. Rev. Lett.* **84**, 5732 (2000)
[6] S Zhu *et al*, *Phys. Rev. Lett.* **91**, 132501 (2003)
[7] R Bengtsson *et al*, *Nucl. Phys.* **A415**, 189 (1984)
[8] R Bengtsson *et al*, *Nucl. Phys.* **A415**, 189 (1984)
[9] H Hubel, *Prog. Part. Nucl. Phys.* **54**, 1 (2005)
[10] S Frauendorf, *Nucl. Phys.* **A557**, 259c (1993)
[11] R M Clark and A O Macchiavelli, *Ann. Rev. Nucl. Part. Sci.* **50**, 1 (2000)
[12] A Chatterjee, Priv. Comm. (2001); http://www.tifr.res.in/∼pell/lamps.html
[13] T Bhattacharjee *et al*, *Nucl. Phys.* **A750**, 199 (2005)
[14] T Bhattacharjee *et al*, *Phys. Rev.* **C78**, 024304 (2008)
[15] T Bhattacharjee *et al*, *Nucl. Phys.* **A825**, 16 (2009)
[16] R K Bhowmik *et al*, *Proceedings of DAE Symposium on Nuclear Physics* **B44**, 422 (2001)
[17] N R Johnson *et al*, *Phys. Rev.* **C55**, 652 (1997) and references therein
[18] G Gangopadhyay *et al*, *Eur. Phys. J.* **A24**, 173 (2005)
[19] M A Rizzutto *et al*, *Z. Phys.* **A344**, 221 (1992)
[20] P Ring and P Schuck, *The nuclear many body problem* (Springer, Berlin, 1980)
[21] W Nazarewicz *et al*, *Nucl. Phys.* **A435**, 397 (1985)
[22] W Nazarewicz, M A Riley and J D Garrett, *Nucl. Phys.* **A512**, 61 (1990)
[23] B A Brown *et al*, The Computer Code 'OXBASH', MSU-NSCL Report No. 524 (June, 1994)
[24] B A Brown *et al*, OXBASH for Windows, MSU-NSCL Report 1289 (2004)
[25] R Bengtsson *et al*, *Nucl. Phys.* **A415**, 189 (1984)
[26] I Hamamoto, *Phys. Lett.* **B235**, 221 (1990)
[27] J R Cooper *et al*, *Phys. Rev. Lett.* **87**, 132503 (2001)
[28] T Bhattacharjee *et al*, *Phys. Rev. Lett.* (communicatied)
[29] Amita, Ashoke Kumar Jain and Balraj Singh, *Atom. Data Nucl. Data Tables* **74**, 283 (2000)
[30] Amita *et al*, Compilation in NNDC, 2006
[31] S Juutinen *et al*, *Phys. Rev.* **C52**, 2946 (1995)
[32] E S Paul *et al*, *Phys. Rev.* **C40**, 1255 (1989)
[33] S Lakshmi *et al*, *Phys. Rev.* **C69**, 014319 (2004)
[34] S Lakshmi *et al*, *Nucl. Phys.* **A761**, 1 (2005)
[35] A O Macchiavelli *et al*, *Phys. Rev.* **C57**, R1073 (1998)
[36] A O Macchiavelli *et al*, *Phys. Lett.* **B450**, 1 (1999)